Received: 25 July 2018 | Revised: 28 September 2018 | Accepted: 4 October 2018

DOI: 10.1002/aoc.4674

WILEY Applied Organometallic Chemistry

FULL PAPER

Carbon-iodide bond activation by cyclometalated Pt (II) complexes bearing tricyclohexylphosphine ligand: A comparative kinetic study and theoretical elucidation

Samira Chamyani[1] | Hamid R. Shahsavari[1] | Sedigheh Abedanzadeh[2] | Mohsen Golbon Haghighi[3] | Sepideh Shabani[1] | Behrouz Notash[3]

[1]Department of Chemistry, Institute for Advanced Studies in Basic Sciences (IASBS), Zanjan 45137-66731, Iran

[2]Institute of Biochemistry and Biophysics (IBB), University of Tehran, Tehran, Iran

[3]Department of Chemistry, Shahid Beheshti University, Evin, Tehran 19839-69411, Iran

Correspondence
Hamid R. Shahsavari, Department of Chemistry, Institute for Advanced Studies in Basic Sciences (IASBS), Zanjan 45137-66731, Iran.
Email: shahsavari@iasbs.ac.ir

Funding information
Institute for Advanced Studies in Basic Sciences (IASBS) Research Council, Grant/Award Number: G2018IASBS32629

Cyclometalated Pt (II) complexes [PtMe(C^N)(L)], in which C^N = deprotonated 2,2′-bipyridine *N*-oxide (Obpy), **1**, deprotonated 2-phenylpyridine (ppy), **2**, deprotonated benzo [h] quinolone (bzq), **3**, and L = tricyclohexylphosphine (PCy_3) were prepared and fully characterized. By treatment of **1–3** with excess MeI, the thermodynamically favored Pt (IV) complexes *cis*-[$PtMe_2I$(C^N)(PCy_3)] (C^N = Obpy, **1a**; ppy, **2a**; and bzq, **3a**) were obtained as the major products in which the incoming methyl and iodine groups adopted *cis* positions relative to each other. All the complexes were characterized by means of NMR spectroscopy while the absolute configuration of **1a** was further determined by X-ray crystal structure analysis. The reaction of methyl iodide with **1–3** were kinetically explored using UV–vis spectroscopy. On the basis of the kinetic data together with the time-resolved NMR investigation, it was established that the oxidative addition reaction occurred through the classical S_N2 attack of Pt (II) center on the MeI reagent. Moreover, comparative kinetic studies demonstrated that the electronic and steric nature of either the cyclometalating ligands or the phosphine ligand influence the rate of reaction. Surprisingly, by extending the oxidative addition reaction time, very stable iodine-bridged Pt (IV)-Pt (IV) complexes [Pt_2Me_4(C^N)$_2$(μ-I)$_2$] (C^N = Obpy, **1b**; ppy, **2b**; and bzq, **3b**) were obtained and isolated. In order to find a reasonable explanation for the observation, a DFT (density functional theory) computational analysis was undertaken and it was found that the results were consistent with the experimental findings.

KEYWORDS
cyclometalated platinum complexes, DFT calculations, kinetic study, oxidative addition, tricyclohexylphosphine ligand

1 | INTRODUCTION

The addition of alkyl halides to square planar metal complexes, via oxidative addition reactions, is still of great interest because of their important role in catalysis and in transition metal mediated organic synthesis.[1–6] On-going investigations continue to develop our understanding of the mechanism of the reaction with the aim of obtaining better rationally designed catalysts in the future.

Platinum (II) complexes provide a useful platform for kinetic and mechanistic studies of fundamental oxidative addition reactions because of their relative inertness, high stability and availability of different oxidation states.[7] Oxidative addition of C–X bonds to platinum (II) complexes is generally enthalpically favored and produces the corresponding platinum (IV) products normally proceeding through a S_N2 type mechanism in which the Pt (II) center acts as a nucleophile *via* the filled d_z^2 orbital.[8,9] However, a radical pathway as well as concerted three-center mechanisms have also been suggested for oxidative addition reactions.[10–12]

Kinetic studies have revealed that the chemical reactivity of platinum complexes depends on the coordination environment around the central metal ions.[13] Π-extended cyclometalating ligands would be expected to offer the metal ion, a strong ligand field and consequently produce significant changes in the physical and chemical properties.[14] In particular, cyclometalated platinum complexes have attracted long-lasting interest due to their potential applications in a wide range of research areas such as organometallic synthesis,[15,16] catalysis,[17,18] organic light-emitting diode (OLED)[19,20] and the design of antitumor agents.[21,22] The C^N-cycloplatinated (II) complexes, where C^N = chelating carbon-nitrogen donor ligand, were found to be reactive substrates for oxidative addition reactions.[23–25]

Accordingly, the nature of ancillary ligands can strongly controls the lability of platinum complexes. With regard to recent reports, the investigations based on the oxidative addition of alkyl halides to platinum complexes, were carried out using complexes with nitrogen donor ligands,[26–28] and phosphine-ligated platinum (II) analogs have received less attention.[29] However, phosphine ligands effectively provide a wide range of attractive features for the platinum complexes, by inducing specific electronic and steric properties. Therefore, there is still great interest in synthesizing and evaluating the reactivity of platinum phosphine complexes, due to their potential applications in many active research areas.[30,31]

Following our interest on the reaction kinetics of oxidative addition of cycloplatinated (II) complexes,[32–35] in the present study, a series of cyclometalated Pt (II) complexes with general formula [PtMe(C^N)(L)], were designed to be synthesized with different C^N-cyclometalating ligands (C^N = deprotonated 2,2′-bipyridine *N*-oxide, **1**,[30] deprotonated 2-phenylpyridine, **2** and deprotonated benzo [h] quinolone, **3** while including tricyclohexylphosphine (PCy_3) as the monodentate phosphine ligand (L). Afterwards, the oxidative addition reaction of MeI, one of the promising haloalkanes, with the cyclometalated Pt (II) complexes was investigated by a combination of experimental and theoretical methods, and the differences in reactivity compared. The major aim of this research was to enhance our understanding of the effect of the ligand system on the reactivity of cycloplatinated (II) complexes, both from the synthetic and kinetico-mechanistic points of view.

2 | RESULT AND DISCUSSION

2.1 | Synthesis and characterization

The synthetic route for the preparation of cyclometalated Pt (II) and Pt (IV) complexes is summarized in Scheme 1.

Methylplatinum (II) complexes [PtMe(C^N)(PCy_3)], C^N = deprotonated 2,2′-bipyridine *N*-oxide (Obpy), **1**,[30] deprotonated 2-phenylpyridine (ppy), **2**, and deprotonated benzo [h] quinolone (bzq), **3**, were synthesized by the reaction of starting complexes [PtMe(C^N)(SMe_2)], C^N = Obpy, **A**[36]; ppy, **B**[37]; and bzq, **C**,[38] with tricyclohexylphosphine (PCy_3) ligand as the monodentate P-donor ligand. The dimethyl sulfide (SMe_2) ligands easily displaced with an equimolar quantity of PCy_3 at room temperature. The new synthesized complexes were characterized by NMR spectroscopy. $^{31}P\{^1H\}$ NMR spectra display a sharp singlet signal with platinum satellites at 22.2, 23.4 and 24.2 ppm, for complexes **1–3**, respectively, confirming the presence of Pt (II)-bound PCy_3 ligands. The coupling constants of $^1J_{PtP}$ = 2162 Hz (**1**),[30] 1937 Hz (**2**) and 2052 Hz (**3**) are typical for the P-*trans*-C (sp^2) geometry.[39] It is noteworthy that this significant difference in the coupling values of $^1J_{PtP}$ (about 120 Hz), is attributed to the *trans* influence of coordinated carbon atom of the C^N-cyclometalated ligands (Obpy > bzq > ppy).[40] The $^{195}Pt\{^1H\}$ NMR spectra of these complexes contain a doublet resonance with a

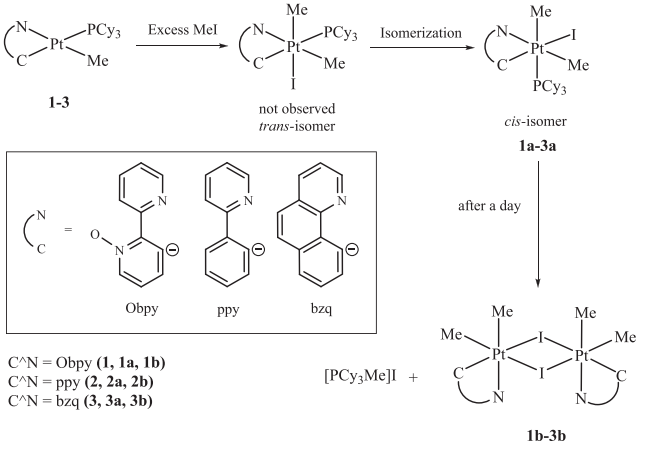

SCHEME 1 Synthetic route for preparation of cyclometalated Pt (II) complexes with the PCy_3 ligand and their oxidative addition reaction with MeI

coupling constant value that is almost equal to that observed in the corresponding $^{31}P\{^1H\}$ NMR spectra. In the ^1H NMR spectra of these complexes, protons of Pt-coordinated methyl ligand appear as doublet resonances with the Pt satellites at 0.83–1.07 ppm, which coupled with both phosphorus and platinum nuclei. Additionally, the characteristic protons of cyclohexyl substituents of the PCy_3 were detected at 1.20–2.60 ppm, in the aliphatic region of the ^1H NMR spectra. Also, in the $^{13}C\{^1H\}$ NMR spectra the carbon atom of the methyl group in **1–3** appears as a doublet signal ($\delta = -14.9$ to -16.0 ppm) due to coupling with the phosphorus atom and the Pt center ($^2J_{PC}$ = 6–7 Hz, $^1J_{PtC}$ = 752–763 Hz).[30] All the NMR spectra (Figures S1–S8) for the new Pt (II) complexes together with the NMR labelling (Scheme S1) is available in the Supporting Information. Furthermore, the numerical NMR data are also reported with detail in the Experimental section.

The methylplatinum (II) complexes, **1–3**, were treated with an excess of methyl iodide in CH_2Cl_2 at room temperature to yield the corresponding Pt (IV) products with the general formula *cis*-[$PtMe_2I$(C^N)(PCy_3)] (C^N = Obpy, **1a**; ppy, **2a**; and bzq, **3a**). The NMR spectra (Figures S9-S20) provide precise information about the reaction process. In the ^1H NMR spectra, a new doublet signal with platinum coupling was observed corresponding to the new incoming Me group. Protons of cyclohexyl moieties in PCy_3, as well as two Pt (IV)-bound methyl groups (Me *trans* to N and Me-*trans*-P) appeared as overlapping multiplets in the aliphatic region of ^1H NMR spectra. $^{31}P\{^1H\}$ NMR spectra displayed a singlet resonance in shielded region, coupled with ^{195}Pt center which was related to the phosphorus atom adjacent to the Pt (IV) center. These signals were observed at −19.4 ppm (**1a**), −18.0 ppm (**2a**) and − 17.9 ppm (**3a**) with $^1J_{PtP}$ coupling constants of $^1J_{PtP}$ = 955, 956 and 963 Hz, respectively, indicative of Pt (IV)-bound phosphorus nuclei. The $^{195}Pt\{^1H\}$ NMR spectra of these complexes possess a doublet at −3215.1 ppm with $^1J_{PPt}$ = 957 Hz (**1a**), −3175.7 ppm with $^1J_{PtP}$ = 953 Hz (**2a**) and − 3201.6 with $^1J_{PtP}$ = 968 Hz (**3a**), which are almost in conformance with the coupling constant observed in the $^{31}P\{^1H\}$ NMR spectra. As can be seen, the coupling constant values of Pt (IV) products are almost the same while in the case of corresponding Pt (II) complexes **1–3** the values attained for $^1J_{PtP}$, showed significant differences deriving from different *trans* influence of the bridgehead carbon atom in each C^N ligand (Obpy, ppy, bzq). In the $^{13}C\{^1H\}$ NMR spectra of Pt (IV) complexes, the carbon of both methyl ligands (*trans* to N or *trans* to P) in **1a-3a** exhibit a doublet with a large coupling constant value to platinum center ($^1J_{PtC}$). Also, the aromatic regions in these spectra are almost similar to those of their Pt (II) derivatives with only smaller coupling constants for the Pt (IV) center in relation to their Pt (II) parents. This observation is due to the increasing in the oxidation state of the platinum center from +2 to +4 during the oxidative addition reaction which can be related to a formal change of hybridation state from dsp^2 to d^2sp^3.[33] The results confirm that the phosphine ligand (PCy_3) is placed in the mutual *trans* position relative to the Me ligand, in any of the Pt (IV) products.[34] As a consequence, the complexes **1a-3a** were obtained almost quantitatively as thermodynamically stable complexes displaying *cis* disposition of Me and I ligands.

As will be discussed later, density functional theory (DFT) calculations highlighted the larger stabilization of Pt (IV) complex with the *cis* arrangement of incoming Me and I ligands, over the corresponding *trans* analogue. In fact, the tricyclohexylphosphine ligand with large cone angle value,[41] is considered to impose steric constraints when located in an equatorial site of complex. Therefore, the thermodynamically more stable product is preferentially formed and the PCy_3 ligand is situated in the axial position, being introduced as the *cis* product.

Complex **1a** was structurally characterized by single crystal X-ray crystallography method. The appropriate crystals were grown by slow diffusion of *n*-hexane into the CH_2Cl_2 solution of complex. It was found to crystallize in the monoclinic crystal system in space group $P2_1/c$. The crystal data and structural refinement parameters are summarized in Table S1. The ORTEP view of **1a** is illustrated in Figure 1 which shows that the Pt (IV) center adopts an octahedral coordination geometry with the PCy_3 ligand in an axial site. The X-ray crystal structure confirms the formation of thermodynamically favored *cis* isomer for this complex. As shown in Figure 1, Pt (IV) center adopts a slightly distorted octahedral environment, surrounded by carbon-nitrogen donor atoms of the Obpy ligand (C1, N2), a carbon atom of Me ligand (Cl2) and an iodine atom (I1) while the other Me group (Cl1) besides the PCy_3 moiety (P1) situated in the axial positions. The dihedral angle between the aromatic rings of the cyclometalated Obpy ligand is 7.4° which is in good agreement with previous reports.[34,42]

The reaction mixtures were kept at room temperature over time. After one day, very stable Pt (IV)–Pt (IV) complexes of formula [Pt_2Me_4(C^N)$_2$(μ-I)$_2$], (C^N = Obpy, **1b**; ppy, **2b**; and bzq, **3b**[43]) were detected along with the equimolar amounts of [PCy_3Me]I[32] (Scheme 1). Dinuclear cycloplatinated (IV) complexes with two iodine atoms as bridging ligands have been generated by complete removal of the monophosphine PCy_3 ligands. Similar observations have been reported in previous studies.[35,43] NMR spectroscopy provided clear evidence on the formation of complexes **1b-3b** (Figures S21-S29). The characteristic signals related to the PCy_3 ligands disappeared in both the ^1H and $^{31}P\{^1H\}$ NMR spectra. In

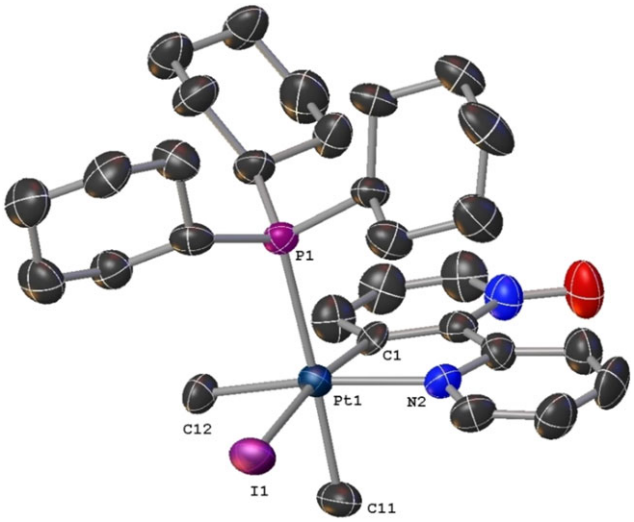

FIGURE 1 ORTEP plot of the structure of **1a** with its atom labeling scheme. Selected bond lengths (Å) and angles (deg): Pt1-C1 1.994(8), Pt1-C11 2.095(10), Pt1-C12 2.103(8), Pt1-N2 2.150(8), Pt1-I1 2.7694(10), Pt1-P1 2.509(2), C11-Pt1-P1 177.2(3), C1-Pt1-I1 172.1(3), C12-Pt1-N2 168.3(3), C1-Pt1-N2 79.2(3), C1-Pt1-C11 85.8(4), C12-Pt1-I11 88.0(3). Ellipsoids are drawn at the 40% probability level, and hydrogen atoms are eliminated for clarity

the ^{1}H NMR spectra, two distinctive singlet resonances flanked with Pt satellites at 1.10–1.20 and 1.40–170 ppm which were assigned to the Me groups *trans*-positioned to I and N, respectively. Additionally, $^{31}P\{^{1}H\}$ NMR spectroscopy revealed a sharp singlet signal at 33.7 ppm for isolated [PCy_3Me] I while in the ^{1}H NMR spectrum, the aliphatic protons appeared as multiplets that overlapped with each other. The $^{195}Pt\{^{1}H\}$ NMR spectra of **1b-3b** contains a clear singlet which confirmed both platinum centers in these complexes are equivalents. With regard to the $^{13}C\{^{1}H\}$ NMR spectra for **1b-3b**, two sets of signals for the methyl groups (*trans* to N or *trans* to I) appeared in the aliphatic region. In order to provide a proper explanation about the reaction route, DFT computational method was applied and results are ascribed in later sections.

2.2 | Kinetic and mechanism study

The oxidative addition reaction of MeI with complexes **1**–**3** were monitored in CH_2Cl_2 using UV–vis spectroscopy. An excess of MeI was added, so that its concentration can be considered to be constant during each kinetic run. The distinctive MLCT (metal to ligand charge transfer) bands of the Pt (II) complexes gradually disappeared with addition of excess MeI while oxidative addition reaction occur. Figure 2 represents the changes in UV–vis spectra of **1**–**3** at 298 K. In order to obtain pseudo-first-order rate constants (k_{obs}), the absorbance-time profiles

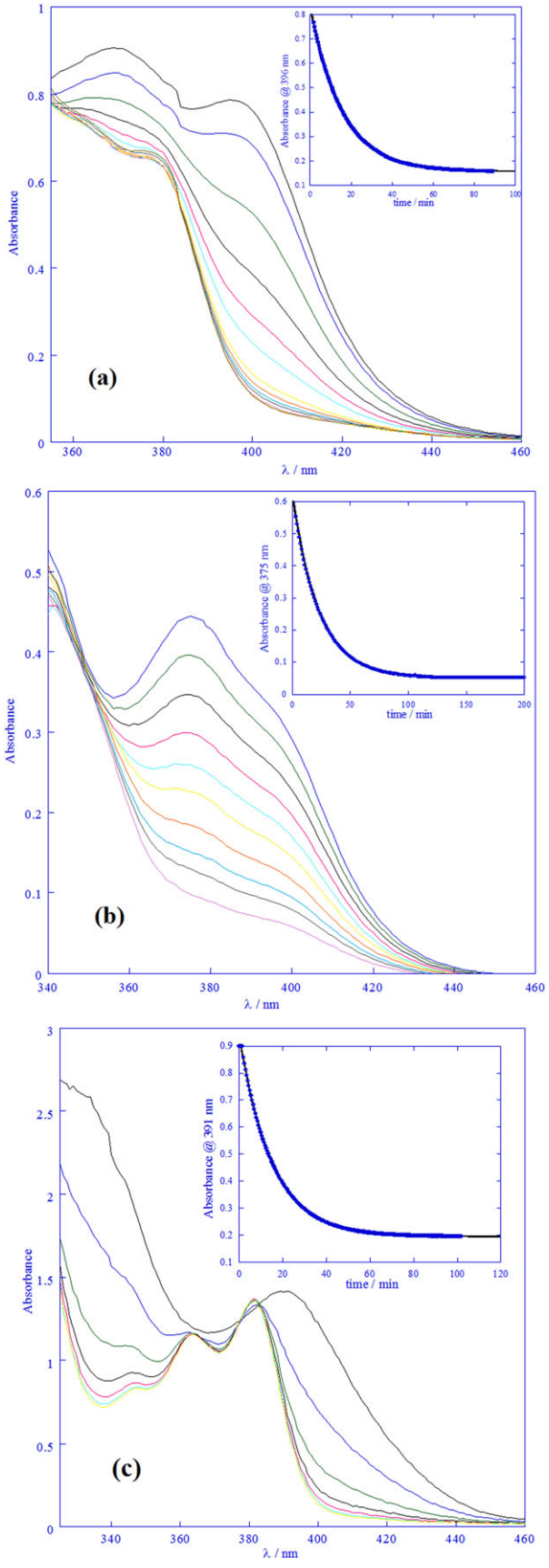

FIGURE 2 Changes in the UV–vis spectrum of (a) **1**, (b) **2** and (**3**) with MeI in CH_2Cl_2 at 25 °C (the inset shows the variation of the absorbance at the corresponding wavelength over time)

were fitted to a first-order equation by nonlinear least-squares techniques. Figure 3 shows the linear plots of calculated k_{obs} values against the concentration of MeI with no intercepts, providing information on the first-order dependence of the rate upon the MeI concentration. The slope of each straight line is indicative of the second-order rate constant (k_2).

Based on the kinetically data, all of the reactions follow second-order rate law, first order in either the Pt (II) complex and the MeI reagent, following a classical S_N2 oxidative addition mechanism. Similar experiments were carried out in different temperatures. All the attained k_2 values related to the Pt (II) complexes are collected in Table 1. The activation parameters, $\Delta H^{\#}$ = enthalpy and $\Delta S^{\#}$ = entropy of activation, were calculated using the Eyring equation (Figure 4) and are also summarized in Table 1. The large negative value of $\Delta S^{\#}$ obtained for each reaction is the best evidence for suggesting S_N2 pathway.

The reaction rates of complexes **1**–**3** with MeI, proceed in the order **2** > **3** > > **1**. For instance, the oxidative addition of MeI to **2** was found to be faster than that of **1**, but the reaction rate of **3** is near to the reaction rate of **2**. This result is attributed to the relatively lower reactivity of **1** when compared to **2** or **3**. When the oxidative addition reaction of MeI to the Pt (II) complexes goes through the S_N2 mechanism, the Pt (II) center nucleophilically attacks at the methyl group of MeI, confirming the associative nature of reaction. Indeed, a more electron-rich metal center would react faster in this step. The different electronic effects of the C^N ligands, evidently influences the lability of the Pt (II) complex. Cyclometalating ligands with electron-withdrawing substituents lead the platinum center to be less electron-dense and consequently less reactive toward the oxidative addition reaction. Thus, the observed trend for the rate constant of complexes (**2** > **3** > > **1**) is consistent with the trend of the donor ability of the supporting ligands as 2,2′-bipyridine *N*-oxide (Obpy-H) donates less electron density to the platinum center when compared to 2-phenylpyridine (ppy-H) or benzo [h] quinolone (bzq-H). Notice that the formation rate of kinetically favored *trans* isomers, resulting from the *trans* addition of MeI to the Pt (II) center, also shows the same trend. The more electron-rich metal center, certainly produces the related *trans* product faster.

It should be noted that the kinetic product was initially produced due to the intrinsic tendency of MeI for mutual *trans* coordination but the large steric demand of PCy_3[41] makes the kinetic product unstable enough to rapidly convert to the stable *cis* product. As a result, complexes **1a**-**3a** having the Me and I in *cis* dispositions, were synthesized, whereas no *trans* isomers were isolated. As aforementioned, the steric character of phosphine ligand strongly controls the rate of the oxidative addition reaction. Ligands with sterically bulk substituents enhance the rate of the *trans-cis* transformation that is generally occurs to afford the thermodynamically stable product in which incoming methyl and iodine groups occupy *cis* positions relative to each other. Therefore, the rate of oxidative addition reactions are greatly dependent on the characteristics of coordinated ligands.

The proposed mechanism is depicted in Scheme 2. The oxidative addition reaction initiated by the nucleophilic attack of Pt (II) center to the methyl group of MeI. The cationic intermediate is formed and subsequently transform to the new intermediate by pseudo-rotation.[44] Eventually, the corresponding thermodynamic Pt (IV) complex is obtained by the coordination of iodine to the *cis* vacant site of platinum center. It is believed that the final product is more thermodynamically stable than the experimentally non-observed kinetic product.

2.3 | NMR monitoring

In order to better understand about the details of the reaction, NMR spectroscopy was applied to monitor the process. Complex **1** was reacted with excess amounts of CH_3I in CD_2Cl_2 in the NMR tube and the reaction was followed up using ^1H and $^{31}P\{^1H\}$ NMR spectroscopies at room temperature (Figure 5). Addition of MeI immediately resulted in the formation of singlet signal with Pt satellite at $\delta = -19.4$ ppm, along with the disappearance of the singlet resonance of Pt (II) complex, **1**, at $\delta = 22.2$ ppm. The new signal, appeared in the shielded region, was assigned to the thermodynamically stable product **1a**, with a *cis* arrangement of the Me and I ligands. As stated previously, sterically-hindered the PCy_3 ligand in the *trans* Pt (IV) product, caused the *trans* isomer rapidly converts to the stable *cis* isomer. Thus, due to the very fast interconversion process, the kinetic product could not be detected in the NMR spectrum. According to the recorded NMR spectra, the intensity of the resonance related to *cis* isomer gradually increased with time. As the reaction progressed, the NMR monitoring revealed the appearance of a new singlet signal at $\delta = 33.7$ ppm while the characteristic resonances of *cis* isomer started to fade. On the basis of observations, the growing signal was assigned to the [PCy_3Me] I species, which has been formed by the reaction of dissociated PCy_3 with free MeI reagents during the reaction.

Accordingly, the ^1H NMR study provided the same data which obtained from the $^{31}P\{^1H\}$ NMR spectra. The distinctive signal at $\delta = 0.90$ ppm (due to the coordinated Me group in **1**) was used to monitor the reaction.

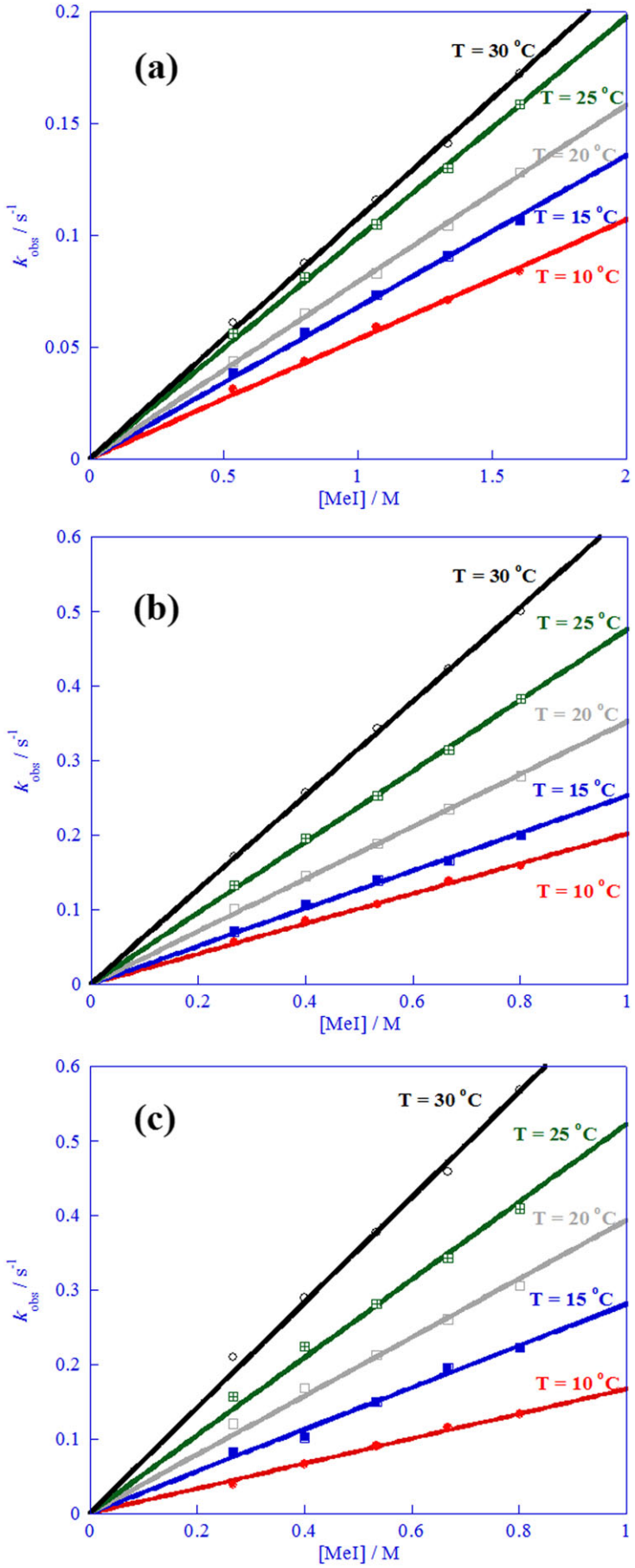

FIGURE 3 Plots of the first-order rate constants (k_{obs}/s^{-1}) for the reaction of (a) **1**, (b) **2** and (**3**) with MeI in CH_2Cl_2 at different temperatures *versus* the MeI concentration

TABLE 1 Second-order rate constants and activation parameters[b] for the reaction of complexes **1–3** with MeI in CH_2Cl_2

Complex	C^N	λ_{max}/nm	10^2 k_2/L mol^{-1} s^{-1} at different temperatures					$\Delta H^{\#}$ /kJ mol^{-1}	$\Delta S^{\#}$ /JK^{-1} mol^{-1}
			10 °C	15 °C	20 °C	25 °C	30 °C		
1	Obpy	396	0.9	1.11	1.32	1.55	1.82	39.2 ± 0.1	−96 ± 1
2	ppy	375	1.64	1.92	2.37	2.81	3.36	34.1 ± 0.2	−109 ± 1
3	bzq	391	1.57	1.79	2.28	2.66	3.24	35.6 ± 0.1	−102 ± 2

Estimated errors in k_2 values are ±3%.

[b]Activation parameters were calculated from the temperature dependence of the second-order rate constant in the usual way using Eyring equation ($\ln(k_2/T) = \ln(k_B/h) - \Delta H^{\neq}/RT + \Delta S^{\neq}/R$).

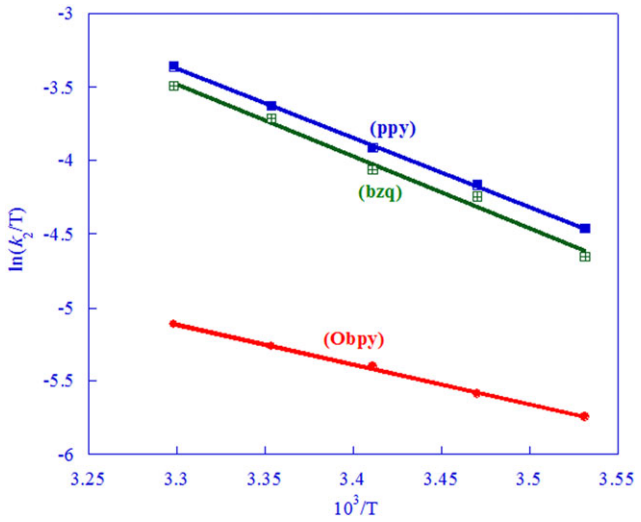

FIGURE 4 Eyring plots for the reactions of **1–3** with MeI in CH_2Cl_2

However, new resonances started to appear when the reaction was progressed. Based on the ^{1}H NMR data, by prolonging the reaction time, the phosphine ligand started to leave the Pt (IV) *trans* product and ultimately, the stable dinuclear complex with the formula $[Pt_2Me_4(Obpy)_2(\mu\text{-}I)_2]$, **1b**, was formed while two iodine ligands join two Pt (IV) centers together. In addition, an equimolar amount of $[PCy_3Me]$ I species were simultaneously produced.

2.4 | Theoretical calculations

DFT calculations were utilized in order to gain further insights into the reaction mechanism. Computed structures are depicted in Figure 6 with their respective relative energy values in kJ mol^{-1} for the oxidative addition reaction involving **1** with MeI. The result of the theoretical calculations are in close agreement with the experimental observations.

According to the empirical kinetic studies, the oxidative addition of MeI to Pt (II) complexes proceeded through the S_N2 reaction pathway as can be observed in Scheme 2. The nucleophilic attack of the Pt (II) center on the carbon atom of the MeI reagent was proposed to promote the reaction path resulting in the formation of the initial product in which incoming methyl and iodine

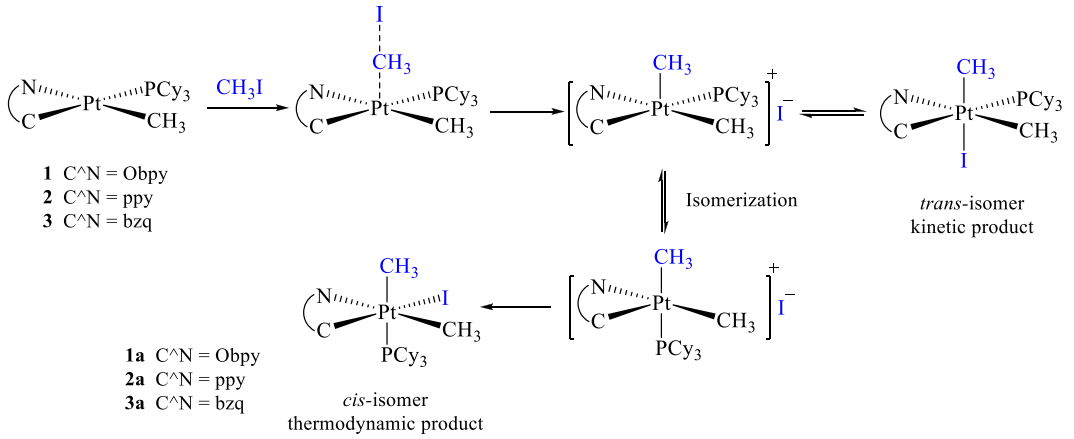

SCHEME 2 Proposed S_N2 mechanism for the oxidation of **1–3**

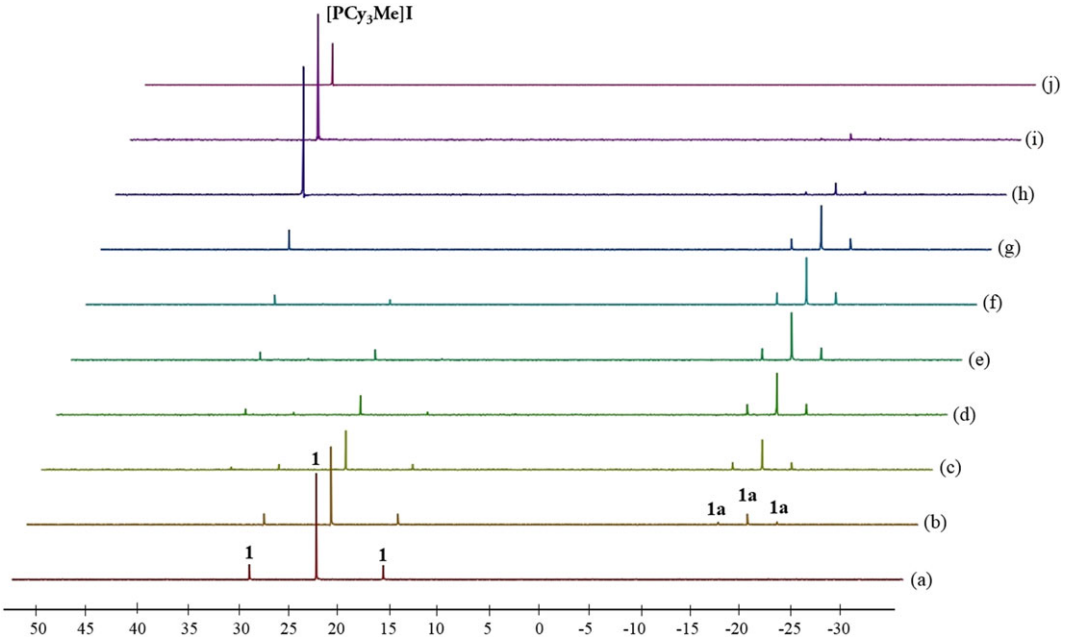

FIGURE 5 The reaction of **1** with an excess of MeI (30 folds) as monitored by $^{31}P\{^{1}H\}$ NMR spectroscopy in CD_2Cl_2 at room temperature. (a) pure complex **1**, (b) immediately, (c) 10 min, (d) 20 min, (e) 30 min, (f) 40 min, (g) 110 min, (h) 1 day, (i) 2 days after addition of excess MeI and (j) pure $[PCy_3Me]I$. The signal assignments are depicted

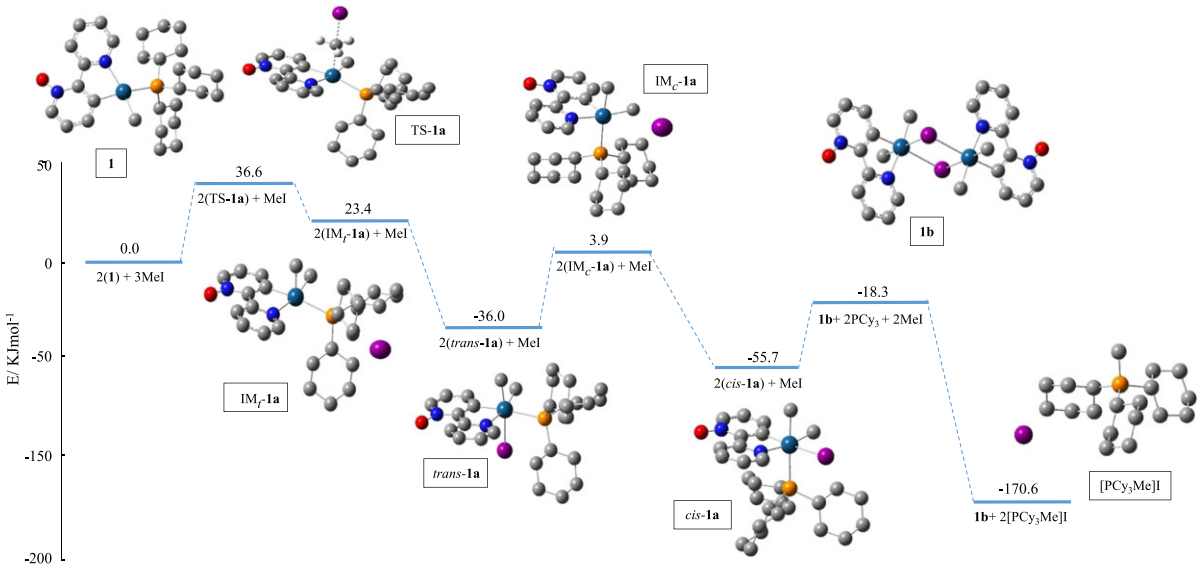

FIGURE 6 Relative energies (kJ mol^{-1}) for products and intermediates arising from the addition of MeI to **1** in CH_2Cl_2

groups occupy *trans* positions relative to each other. Afterward, the kinetic product promptly converted to the thermodynamic *cis* isomer, because of the significant steric hindrance of the phosphine ligand (PCy_3). Based on the calculated energy profile which indicated in Figure 6, the kinetically favored product is at higher energy by comparison to the alternative thermodynamic isomer. Therefore, DFT calculations parallel to experiments, demonstrated that Pt (IV) products with *cis* geometry, were found to be more stable than related *trans* isomers. The nucleophilic attack of $5d_Z^2$ atomic orbital of Pt (II) center on the σ* of Me-I results in the formation of a transition state entity (TS-**1a**) in which the Pt-C (Me)-I angle is close to 180° demonstrating a linear structure with a planar Me at the center. In this structure, methyl is approaching the metal center while the C-I bond is gradually being broken which finally leads to the formation of cationic IM_t-**1a** intermediate possessing a distorted square pyramidal

geometry (incoming methyl is located on the apical position). This intermediate can be converted to the *trans* kinetic product (*trans*-**1a**) or rearranged to cationic IM_c-**1a** intermediate which are theoretically more stable than its IM_t-**1a** parent. It seems to be logical that the IM_c-**1a** energy level is lower than that of IM_t-**1a** intermediate because the IM_c-**1a** intermediate is eventually transformed to the more stable *cis* product (*cis*-**1a**) rather than IM_t-**1a** intermediate.

By extending the reaction time, the stable iodine-bridged cycloplatinated complex **1b** has been formed accompanied with the equimolar quantities of $[PCy_3Me]I$ species. Interesting features were emerged by analyzing the theoretical investigations. Activation barriers calculated revealed that the enthalpy value obtained for the formation of dinuclear Pt (IV)-Pt (IV) complex **1b** together with $[PCy_3Me]I$ species, is significantly smaller than that of Pt (IV) complex **1a**. The greater stability of **1b** along with the formation of $[PCy_3Me]I$ promotes the reaction over time. While, it appears that the intermediate (**1b** + 2MeI + $2PCy_3$) lies in levels above the reactants (**1a** + MeI), DFT studies clearly show that the thermodynamic preference for **1b** + $[PCy_3Me]I$. Hence, when the reaction is in progress for a day, it is reasonable to observe the formation of the dinuclear Pt (IV)-Pt (IV) complex **1b**.

3 | CONCLUSION

This study presents an empirical and theoretical about the oxidative addition reaction of methyl iodide to cyclometalated Pt (II) complexes bearing phosphine ligands. In summary, cyclometalated Pt (II) complexes $[PtMe(C\hat{}N)(PCy_3)]$, including tricyclohexylphosphine (PCy_3) ligand, for which C^N = deprotonated 2,2′-bipyridine *N*-oxide (Obpy, **1)**, deprotonated 2-phenylpyridine (ppy, **2**) and deprotonated benzo [h] quinolone (bzq, **3**) were prepared and readily characterized by multinuclear NMR techniques. The reaction kinetics of excess MeI with the cyclometalated Pt (II) phosphine complexes were accurately determined by analyzing the UV–vis spectra. Kinetic results as well as calculated activation parameters, illustrated that the reactions goes through the S_N2 pathway, following the second order kinetic rate law. In addition, it was found that the rate-determining step of reaction processes is highly dependent on the metal coordination architecture. The significantly greater electron-withdrawing character of the Obpy cyclometalating ligand in comparison with ppy, makes the Pt (II) center less electron rich toward the nucleophilic attack and accordingly, decreases the rate of oxidative addition reaction with MeI. As previously discussed, after the addition of excess MeI to the solution of complexes **1–3**, Pt (IV) complexes possessing a general formula of *cis*-$[PtMe_2I(C\hat{}N)(PCy_3)]$ (C^N = Obpy, **1a**; ppy, **2a**; and bzq, **3a**) were exclusively obtained and isolated. As confirmed by DFT computational method, the primarily formed kinetic product with *trans* arrangement of incoming Me and I groups, prefers to transform to the more stable thermodynamic product with *cis* geometry, certainly due to the steric hindrance of tricyclohexylphosphine ligand. A close examination of NMR monitoring experiment, also indicated that the isomerization process was so fast that the initial oxidative addition of MeI to Pt (II) center, could not be detected. All new complexes were spectroscopically characterized while the six-coordinate Pt (IV) structure of **1a** was successfully determined by X-ray crystallography. Unexpectedly, prolonging the reaction time to one day, caused to produce Pt (IV)-Pt (IV) complexes $[Pt_2Me_4(C\hat{}N)_2(\mu\text{-}I)_2]$ (C^N = Obpy, **1b**; ppy, **2b**; and bzq, **3b**) with bridging iodide ligands accompanied by eqiumolar amount of $[PCy_3Me]I$. DFT computations fully supported the empirical results and interpreted the reaction preference to progress over time due to the large stabilization of iodine-bridged complexes.

4 | EXPERIMENTAL

4.1 | General procedures and materials

Multinuclear ^1H, $^{13}C\{^1H\}$, $^{31}P\{^1H\}$ and $^{195}Pt\{^1H\}$ NMR spectra were recorded on a Bruker Avance DPX 400 MHz instrument. All chemical shifts are reported in ppm (part per million) relative to their corresponding external standards ($SiMe_4$ for ^1H and ^{13}C, 85% H_3PO_4 for ^{31}P and Na_2PtCl_6 for ^{195}Pt) and also all the coupling constants (*J* values) are given in Hz. The microanalyses were performed using a vario EL CHNS elemental analyzer. The UV–vis absorption spectra were carried out using an Ultrospec 3100 Pro UV–vis spectrometer with temperature controlling system by a Pharmacia Biotech constant-temperature bath. All the reactions were performed using commercially available chemicals without any purification. 2-Phenylpyridine (Hppy), benzo [h] quinolone (Hbzq), 2,2′-bipyridine *N*-oxide (HObpy), tricyclohexylphosphie (PCy_3) and MeI were purchased from Sigma-Aldrich chemical. The starting complexes $[PtMe(C\hat{}N)(SMe_2)]$, C^N = (Obpy,[36] ppy[37] and bzq[38]), $[PtMe(k^2N,C\text{-}bipyO\text{-}H)(PCy_3)]$ (**1**)[30] and $[PtMe_4(k^2N,C\text{-}bzq)_2(\mu\text{-}I)_2]$ (**3b**)[43] were prepared according to our previous reports.

4.2 | Synthesis of the Pt (II) complexes

Tricyclohexylphosphine, PCy_3, (0.1 mmol) was added to a solution of starting complexes with general formula of $[PtMe(C\hat{}N)(SMe_2)]$, C^N = Obpy, **A**[36]; ppy, **B**[37]; and

bzq, **C**,[38] (0.1 mmol) in acetone (15 mL), and the solution was stirred for 2 hr. Light yellow solids precipitated, which were separated, washed with cold acetone, and dried under vacuum.

4.2.1 | [PtMe(k^2N,C-ppy)(PCy_3)] (2)

Yield: 76%. Elem. anal. Calcd for $C_{30}H_{44}NPPt$ (644.73); C, 55.89; H, 6.88; N, 2.17. Found: C, 55.76; H, 6.82; N, 2.26. ^{1}H NMR (400 MHz, $CDCl_3$): δ = 1.07 (d, $^3J_{PH}$ = 5.3 Hz, $^2J_{PtH}$ = 84.5 Hz, 3H, PtMe), 1.20–1.40 (m, 9H, Cy), 1.65 (m, 6H, Cy), 1.70–1.90 (m, 9H, Cy), 1.97–2.14 (m, 6H, Cy), 2.36 (m, 3H, Cy), 7.09 (m, 1H, $H^{4'}$), 7.16 (t, 1H, $^3J_{HH}$ = 7.3 Hz, $H^{5'}$), 7.35 (td, 1H, $^3J_{HH}$ = 7.3 Hz, $^4J_{HH}$ = 2.9 Hz, $^4J_{PtH}$ = 29.7 Hz, H^5), 7.70 (bd, 1H, $^3J_{HH}$ = 7.8, H^4), 7.85 (m, 2H, H^3 and $H^{6'}$), 7.95 (dd, 1H, $^3J_{HH}$ = 6.3 Hz, $^4J_{HH}$ = 1.1 Hz, $^3J_{PtH}$ = 46.8 Hz, $H^{3'}$), 8.84 (d, 1H, $^3J_{HH}$ = 5.6 Hz, $^3J_{PtH}$ = 18.3 Hz, H^6); $^{13}C\{^1H\}$ NMR (101 MHz, $CDCl_3$): δ = −15.3 (d, $^2J_{PC}$ = 6 Hz, $^1J_{PtC}$ = 763 Hz, PtMe), 26.7 (s, C of PCy_3), 28.1 (d, $^3J_{PC}$ = 10 Hz, C of PCy_3), 30.0 (s, $^3J_{PtC}$ = 12 Hz, C of PCy_3), 32.9 (d, $^1J_{PC}$ = 21 Hz, $^2J_{PtC}$ = 19 Hz, C of PCy_3), 119.1 (s, $^3J_{PtC}$ = 17 Hz, C^3), 121.8 (s, $^3J_{PtC}$ = 21 Hz, C^5), 123.8 (s, $C^{5'}$), 124.9 (d, $^4J_{PC}$ = 5 Hz, $^3J_{PtC}$ = 16 Hz, $C^{6'}$), 129.8 (d, $^4J_{PC}$ = 6 Hz, $^3J_{PtC}$ = 24 Hz, $C^{4'}$), 132.2 (d, $^3J_{PC}$ = 11 Hz, $^2J_{PtC}$ = 81 Hz, $C^{3'}$), 136.9 (s, C^4), 147.7 (s, $C^{1'}$), 152.0 (s, $^2J_{PtC}$ = 37 Hz, C^6), 164.7 (d, $^2J_{PC}$ = 37 Hz, $C^{2'}$), 167.4 (s, C^2);. $^{31}P\{^1H\}$ NMR (162 MHz, $CDCl_3$): δ = 23.4 (s, $^1J_{PtP}$ = 1937 Hz, 1P of PCy_3); $^{195}Pt\{^1H\}$ NMR (86 MHz, $CDCl_3$): δ = −4043.3 (s, $^1J_{PtP}$ = 1938 Hz, 1Pt).

4.2.2 | [PtMe(k^2N,C-bzq)(PCy_3)] (3)

Yield: 81%. Elem. anal. Calcd for $C_{32}H_{44}NPPt$ (668.75); C, 57.47; H, 6.63; N, 2.09. Found: C, 57.31; H, 6.69; N, 2.21. ^{1}H NMR (400 MHz, $CDCl_3$): δ = 0.83–2.61 (3H of Me and 33H of Cy), 7.46 (dd, 1H, $^3J_{HH}$ = 7.9 Hz, $^3J_{HH}$ = 7.8 Hz, H^8), 7.56 (d, 1H, $^3J_{HH}$ = 8.1 Hz, H^6), 7.67 (d, 1H, $^3J_{HH}$ = 8.1 Hz, H^5), 7.74 (m, 1H, H^3), 7.82 (d, 1H, $^3J_{HH}$ = 8.7 Hz, H^7), 8.23 (dd, 1H, $^3J_{HH}$ = 7.1 Hz, $^3J_{PtH}$ = 45.5 Hz, H^9), 8.34 (d, 1H, $^3J_{HH}$ = 8.3 Hz, H^4), 9.15 (d, 1H, $^3J_{HH}$ = 5.3 Hz, $^4J_{HH}$ = 1.1 Hz, $^3J_{PtH}$ = 17.2 Hz, H^2); $^{13}C\{^1H\}$ NMR (101 MHz, $CDCl_3$): δ = −16.0 (d, $^2J_{PC}$ = 7 Hz, $^1J_{PtC}$ = 754 Hz, PtMe), 26.6 (s, C of PCy_3), 28.2 (d, $^3J_{PC}$ = 10 Hz, C of PCy_3), 30.1 (s, $^3J_{PtC}$ = 11 Hz, C of PCy_3), 32.5 (d, $^1J_{PC}$ = 20 Hz, $^2J_{PtC}$ = 17 Hz, C of PCy_3), 121.1 (s, C^7), 122.3 (s, C^3), 122.9 (s, $C^{5/6}$), 127.2 (s, C^{14}), 129.5 (d, $^4J_{PC}$ = 5 Hz, C^4), 129.9 (s, C^9), 130.0 (s, C^{13}), 130.1 (s, $C^{5/6}$), 134.3 (s, C^{11}), 136.5 (s, C^4), 144.3 (s, C^{10}), 150.4 (s, $^2J_{PtC}$ = 28 Hz, C^2), 163.7 (s, C^{12}); $^{31}P\{^1H\}$ NMR (162 MHz, $CDCl_3$): δ = 24.2 (s, $^1J_{PtP}$ = 2052 Hz, 1P of PCy_3); $^{195}Pt\{^1H\}$ NMR (86 MHz, $CDCl_3$): δ = −4084.9 (s, $^1J_{PtP}$ = 2049 Hz, 1Pt).

4.3 | Reaction of Pt (II) complexes with MeI

An excess amount of MeI (250 μL) was added to a solution of complexes **1–3** in CH_2Cl_2 (15 ml). The reaction mixture was stirred for 1 hr at room temperature and then the solvent was evaporated under reduced pressure. The precipitate was washed with diethyl ether and dried under vacuum to give the product identified as **1a-3a** as pure *cis* isomers.

4.3.1 | *cis*-[$PtMe_2I(k^2$N,C-Obpy)(PCy_3)] (1a)

^{1}H NMR (400 MHz) in $CDCl_3$: δ = 0.86–2.11 (39H, aliphatic region, overlapping multiplets of 2Me and 3Cy), 7.21 (m, 1H, $^3J_{HH}$ = 6.6 Hz, $H^{4'}$), 7.50 (dd, 2H, $^3J_{HH}$ = 6.5 Hz, $^4J_{HH}$ = 2.1 Hz, $^4J_{PtH}$ = 53.1 Hz, H^5 and $H^{3'}$), 8.03 (m, 1H, $^3J_{HH}$ = 7.9 Hz, $^3J_{HH}$ = 7.8 Hz, H^4), 8.22 (d, 1H, $^3J_{HH}$ = 6.5 Hz, $H^{5'}$), 10.09 (d, $^3J_{HH}$ = 5.5 Hz, $^4J_{PtH}$ = 16.1 Hz, 1H, H^3), 10.26 (d, 1H, $^3J_{HH}$ = 7.83 Hz, 1H, H^6); $^{13}C\{^1H\}$ NMR (101 MHz, $CDCl_3$): δ = −7.3 (d, $^2J_{PC}$ = 4 Hz, $^1J_{PtC}$ = 624 Hz, PtMe (Me *trans* to N)), 10.7 (d, $^2J_{PC}$ = 106 Hz, $^1J_{PtC}$ = 461 Hz, PtMe (Me *trans* to P)), 26.3 (s, C of PCy_3), 27.7 (d, $^3J_{PC}$ = 9 Hz, C of PCy_3), 29.2 (s, $^3J_{PtC}$ = 8 Hz, C of PCy_3), 35.7 (d, $^1J_{PC}$ = 14 Hz, $^2J_{PtC}$ = 11 Hz, C of PCy_3), 123.9 (s, $^2J_{PtC}$ = 72 Hz, $C^{3'}$), 126.3 (s, $^3J_{PtC}$ = 7 Hz, C^5), 126.5 (s, $^3J_{PtC}$ = 12 Hz, $C^{4'}$), 127.1 (s, $^2J_{PtC}$ = 14 Hz, C^6), 136.8 (s, C^4), 138.5 (s, C^3), 144.2 (d, $^3J_{PC}$ = 6 Hz, $C^{1'}$), 148.5 (s, $^2J_{PtC}$ = 26 Hz, C^2), 153.7 (s, $^4J_{PtC}$ = 9 Hz, $C^{5'}$), 154.6 (s, $C^{2'}$); $^{31}P\{^1H\}$ NMR (162 MHz, $CDCl_3$): δ = −19.4 (s, $^1J_{PtP}$ = 955 Hz, 1P of PCy_3); $^{195}Pt\{^1H\}$ NMR (86 MHz, $CDCl_3$): δ = −3215.1 (s, $^1J_{PtP}$ = 957 Hz, 1Pt).

4.3.2 | *cis*-[$PtMe_2I(k^2$N,C-ppy)(PCy_3)] (2a)

^{1}H NMR (400 MHz) in $CDCl_3$: δ = 0.85–2.12 (39H, aliphatic region, overlapping multiplets of 2Me and 3Cy), 7.22 (dd, $^3J_{HH}$ = 7.8 Hz, $^3J_{HH}$ = 7.3 Hz, 1H, $H^{4'}$), 7.33 (m, 2H, $H^{5'}$ and $H^{6'}$), 7.50 (d, 2H, $^3J_{HH}$ = 7.8 Hz, $^4J_{PtH}$ = 48.9 Hz, $H^{3'}$), 7.71 (m, 1H, H^4), 7.87 (ddd, $^3J_{HH}$ = 7.5 Hz, $^3J_{HH}$ = 8.0 Hz, $^4J_{HH}$ = 1.3 Hz, 1H, H^5), 7.96 (d, 1H, $^3J_{HH}$ = 8.1 Hz, H^3), 10.12 (d, 1H, $^3J_{HH}$ = 14.8 Hz, H^6); $^{13}C\{^1H\}$ NMR (101 MHz, $CDCl_3$): δ = −7.3 (d, $^2J_{PC}$ = 3 Hz, $^1J_{PtC}$ = 670 Hz, PtMe (Me *trans* to N)), 10.4 (d, $^2J_{PC}$ = 109 Hz, $^1J_{PtC}$ = 469 Hz, PtMe (Me *trans* to P)), 26.4 (s, C of PCy_3), 27.9 (d, $^3J_{PC}$ = 10 Hz, C of

PCy_3), 29.1 (s, $^3J_{PtC}$ = 9 Hz, C of PCy_3), 35.5 (d, $^1J_{PC}$ = 13 Hz, $^2J_{PtC}$ = 10 Hz, C of PCy_3), 119.5 (s, $^3J_{PtC}$ = 11 Hz, C^3), 123.7 (s, $^3J_{PtC}$ = 10 Hz, C^5), 124.2 (s, $^3J_{PtC}$ = 8 Hz, $C^{6'}$), 125.1 (s, $C^{5'}$), 129.3 (s, $^3J_{PtC}$ = 15 Hz, $C^{4'}$), 130.6 (s, $^2J_{PtC}$ = 63 Hz, $C^{3'}$), 137.8 (s, C^4), 141.1 (s, $C^{1'}$), 152.9 (s, $^2J_{PtC}$ = 18 Hz, C^6), 161.8 (s, C^2); $^{31}P\{^1H\}$ NMR (162 MHz, $CDCl_3$): δ = −18.0 (s, $^1J_{PtP}$ = 956 Hz, 1P of PCy_3); $^{195}Pt\{^1H\}$ NMR (86 MHz, $CDCl_3$): δ = −3175.7 (s, $^1J_{PtP}$ = 953 Hz, 1Pt).

4.3.3 | *cis*-[$PtMe_2I(k^2N,C$-bzq)(PCy_3)] (3a)

^1H NMR (400 MHz) in $CDCl_3$: δ = 0.80–2.27 (39H, aliphatic region, overlapping multiplets of 2Me and 3Cy), 7.60–7.85 and 7.88 (m, 6H, aromatic region, overlapping multiplets of bzq), 8.36 (d, 1H, $^3J_{HH}$ = 7.9 Hz, H^4), 10.26 (m, 1H, $^3J_{HH}$ = 5.3 Hz, $^3J_{PtH}$ = 15.5 Hz, H^2); $^{13}C\{^1H\}$ NMR (101 MHz, $CDCl_3$): δ = −7.7 (d, $^2J_{PC}$ = 4 Hz, $^1J_{PtC}$ = 639 Hz, PtMe (Me *trans* to N)), 10.3 (d, $^2J_{PC}$ = 104 Hz, $^1J_{PtC}$ = 476 Hz, PtMe (Me *trans* to P)), 26.3 (s, C of PCy_3), 27.6 (d, $^3J_{PC}$ = 8 Hz, C of PCy_3), 29.0 (s, $^3J_{PtC}$ = 8 Hz, C of PCy_3), 35.6 (d, $^1J_{PC}$ = 15 Hz, $^2J_{PtC}$ = 13 Hz, C of PCy_3), 122.7 (s, C^7), 124.0 (s, $C^{5/6}$), 126.6 (s, $^2J_{PtC}$ = 47 Hz, C^9), 127.5 (s, $^3J_{PtC}$ = 12 Hz, C^{14}), 129.4 (s, C^4), 129.5 (s, C^3), 134.9 (s, $^3J_{PtC}$ = 10 Hz, C^{13}), 136.6 (s, $C^{5/6}$), 137.6 (s, C^{11}), 141.2 (s, C^4), 144.5 (s, C^{10}), 151.3 (s, $^2J_{PtC}$ = 10 Hz, C^2), 151.8 (s, C^{12}); $^{31}P\{^1H\}$ NMR (162 MHz, $CDCl_3$): δ = −17.9 (s, $^1J_{PtP}$ = 963 Hz, 1P of PCy_3); $^{195}Pt\{^1H\}$ NMR (86 MHz, $CDCl_3$): δ = −3201.6 (s, $^1J_{PtP}$ = 968 Hz, 1Pt).

Each reaction mixture containing Pt (II) complex with excess of MeI, was further stirred for 1 day at room temperature in CH_2Cl_2. A white solid precipitated in case **2b** and **3b**, which were separated, washed with cold CH_2Cl_2, and dried under vacuum. In case **1b**, the solvent was removed and the resulting residue was triturated with ether (2 × 3 ml). Complexes **1b-3b** were obtained in the presence of equimolar of [PCy_3Me] I while two components of the mixture were completely separated and characterized (**2b** and **3b**). But for the mixture of **1b** and [PCy_3Me] I, due to high solubility of the complex **1b**, all our attempts were failed and we could not get **1b** in the pure form.

4.3.4 | [$PtMe_4(k^2N,C$-Obpy)$_2(\mu$-I)$_2$] (1b)

^1H NMR (400 MHz) in $CDCl_3$: 0.83–2.70 (aliphatic region, overlapping multiplets), 7.00–8.33 and 9.90–10.47 (aromatic region, overlapping multiplets of 2 Obpy); $^{13}C\{^1H\}$ NMR (101 MHz, $CDCl_3$): δ = −6.7 (s, $^1J_{PtC}$ = 639 Hz, PtMe (Me *trans* to N)), 8.6 (s, $^1J_{PtC}$ = 603 Hz, PtMe (Me *trans* to I)), 123.5 (s, $^2J_{PtC}$ = 65 Hz, $C^{3'}$), 125.5 (s, C^5), 126.6 (s, $C^{4'}$), 126.8 (s, C^6), 136.1 (s, C^4), 137.6 (s, C^3), 145.6 (s, $C^{1'}$), 148.7 (s, $^2J_{PtC}$ = 19 Hz, C^2), 153.5 (s, $C^{5'}$), 154.1 (s, $C^{2'}$); $^{195}Pt\{^1H\}$ NMR (86 MHz, $CDCl_3$): δ = −3019.0 (s, 2Pt).

4.3.5 | [$PtMe_4(k^2N,C$-ppy)$_2(\mu$-I)$_2$] (2b)

^1H NMR (400 MHz) in DMSO-d_6: δ = 1.17 (s, 6H, $^2J_{PtH}$ = 69.54 Hz, Me *trans* to I, PtMe), 1.47 (s, 6H, $^2J_{PtH}$ = 69.64 Hz, Me *trans* to N, PtMe), 7.20–7.45 (6H, overlapping multiplets of $H^{4'}$ and $H^{5'}$ and $H^{6'}$), 7.58 (t, 2H, $^3J_{HH}$ = 6.7 Hz, $H^{3'}$), 8.03 (m, 2H, H^4), 8.15 (2H, $^3J_{HH}$ = 8.3 Hz, H^5), 8.39 (2H, $^3J_{HH}$ = 8.1 Hz, H^3), 9.79 (2H, $^3J_{HH}$ = 5.02 Hz, $^3J_{PtH}$ = 14.4 Hz, H^6); $^{13}C\{^1H\}$ NMR (101 MHz, $CDCl_3$): δ = −5.3 (s, $^1J_{PtC}$ = 631 Hz, PtMe (Me *trans* to N)), −2.3 (s, $^1J_{PtC}$ = 584 Hz, PtMe (Me *trans* to I)), 120.7 (s, $^3J_{PtC}$ = 7 Hz, C^3), 124.9 (s, $C^{5'}$), 125.5 (s, C^5), 126.1 (s, $^3J_{PtC}$ = 17 Hz, $C^{4'}$), 127.5 (s, $^3J_{PtC}$ = 10 Hz, $C^{6'}$), 130.9 (s, $^2J_{PtC}$ = 62 Hz, $C^{3'}$), 139.7 (s, C^4), 141.7 (s, $C^{1'}$), 144.2 (s, $C^{2'}$), 151.3 (s, $^2J_{PtC}$ = 15 Hz, C^6), 160.1 (s, C^2); $^{195}Pt\{^1H\}$ NMR (86 MHz, $CDCl_3$): δ = −2985.3 (s, 2Pt).

4.3.6 | [$PtMe_4(k^2N,C$-bzq)$_2(\mu$-I)$_2$] (3b)

^1H NMR (400 MHz) in DMSO-d_6: δ = 1.17 (s, 6H, $^2J_{PtH}$ = 69.95 Hz, Me *trans* to I, PtMe), 1.65 (s, 6H, $^2J_{PtH}$ = 70.43 Hz, Me *trans* to N, PtMe), 7.56 (d, 2H, $^3J_{HH}$ = 7.2 Hz, $^3J_{PtH}$ = 47.5 Hz, H^9), 7.76 (m, 1H, H^3), 7.87–8.11 (8H, aromatic protons, overlapping multiplets of 2bzq), 8.76 (d, 2H, $^3J_{HH}$ = 8.2 Hz, H^4), 9.98 (d, 1H, $^3J_{HH}$ = 5.2 Hz, $^3J_{PtH}$ = 15.2 Hz, H^2); $^{13}C\{^1H\}$ NMR (101 MHz, $CDCl_3$): δ = −5.9 (s, $^1J_{PtC}$ = 629 Hz, PtMe (Me *trans* to N)), −2.5 (s, $^1J_{PtC}$ = 576 Hz, PtMe (Me *trans* to I)), 124.0 (s, C^7), 124.8 (s, $C^{5/6}$), 122.3 (s, $^3J_{PtC}$ = 16 Hz, C^3), 127.6 (s, $^3J_{PtC}$ = 9 Hz, C^{14}), 128.9 (s, C^4), 129.8 (s, $^2J_{PtC}$ = 63 Hz, C^9), 134.6 (s, $^2J_{PtC}$ = 33 Hz, C^{11}), 137.1 (s, C^{13}), 138.4 (s, $C^{5/6}$), 142.7 (s, C^{10}), 150.0 (s, $^2J_{PtC}$ = 39 Hz, C^{12}), 150.5 (s, $^2J_{PtC}$ = 11 Hz, C^2); $^{195}Pt\{^1H\}$ NMR (86 MHz, $CDCl_3$): δ = −3008.4 (s, 2Pt).

4.3.7 | [PCy_3Me]I

^1H NMR (400 MHz) in CD_2Cl_2: δ = 1.23–2.52 (36H, aliphatic region, overlapping multiplets of Me and 3Cy); $^{31}P\{^1H\}$ NMR (162 MHz, CD_2Cl_2): δ = 33.7 (s, 1P of PCy_3).

4.4 | Single-crystal structure determination

The X-ray diffraction analysis was performed on a STOE IPDS-2/2 T diffractometer equipped using graphite-monochromated Mo Kα radiation. Suitable crystals were

grown by diffusion method and mounted on a glass fiber for further measurements. Diffraction data were collected in a series of ω scans in 1° oscillations and integrated using the Stoe X-AREA[45] software package. A numerical absorption correction was applied using X-RED[46] and X-SHAPE[47] software. The structures were solved by direct methods[48] and then refined on F^2 by a full-matrix least-squares procedure using the X-STEP32 program.[49] All non-hydrogen atoms were refined with anisotropic displacement parameters. Hydrogen atoms were positioned geometrically and constrained as riding atoms with fixed thermal parameters. CCDC-1840636 contains the supplementary crystallographic data for this study.

4.5 | Kinetic measurements

In order to determine the kinetic rate constants of the oxidative addition reaction of MeI with complexes **1–3**, UV–vis spectroscopy was used to follow the changes in the absorbance in CH_2Cl_2. The absorbance-time profiles were derived using pseudo first-order methods. In all measurements, the concentration of the Pt (II) complexes were 3×10^{-4} M in the presence of excess MeI reagent. The collected kinetic data were fitted to the first-order equation (1) to give pseudo first-order rate constants, k_{obs}.

$$Abs_t = Abs_{\infty +} (Abs_0 - Abs_\infty) \exp(-k_{obs} t) \quad (1)$$

The second-order rate constants, k_2, were obtained by determining the slope of the linear plots of k_{obs} against the concentration of the MeI. Similar kinetic experiments have been conducted in different temperatures. $\Delta H^{\neq}$ (activation enthalpy) and $\Delta S^{\neq}$ (activation entropy) parameters were calculated by the Eyring equation (2) where $\Delta H^{\neq}$ = activation enthalpy, $\Delta S^{\neq}$ = activation entropy, k_2 = rate constant, k_B = Boltzmann's constant, T = temperature, h = Planck's constant and R = universal gas constant. All the obtained data are shown in Figures 2, 3 and Table 1.

$$\ln(k_2/T) = \ln(k_B/h) - \Delta H^{\neq}/RT + \Delta S^{\neq}/R \quad (2)$$

4.6 | Kinetic studies using NMR monitoring

The oxidative addition reaction progress was monitored by NMR spectroscopy. Complex **1a** (10 mg) was dissolved in 0.5 ml of CD_2Cl_2 in the NMR tube, and an excess of MeI (30 μL, 30 folds) was added. The NMR spectra were recorded several times at room temperature during about 3 days until the reaction was gradually completed.

4.7 | Computational details

All DFT calculations were employed using the Gaussian09[50] program suite with the B3LYP level of theory. The LANL2DZ[51] basis set was selected to describe Pt and I while the standard 6-31G(d) basis set was utilized for the other atoms. The geometric structures of complexes were optimized by PCM[52,53] model in acetone as the high polar solvent. The vibrational frequency calculations were performed, in order to confirm the nature of the optimized structures.

ACKNOWLEDGMENTS

This work was supported by the Institute for Advanced Studies in Basic Sciences (IASBS) Research Council (G2018IASBS32629). Technical support of the Chemistry Computational Center at Shahid Beheshti University is gratefully acknowledged.

ORCID

Hamid R. Shahsavari http://orcid.org/0000-0002-2579-2185
Mohsen Golbon Haghighi http://orcid.org/0000-0002-2422-9075
Behrouz Notash http://orcid.org/0000-0003-4873-5770

REFERENCES

[1] J. F. Hartwig, *Nature* **2008**, *455*, 314.
[2] P. A. Shaw, J. P. Rourke, *Dalton Trans.* **2017**, *46*, 4768.
[3] M. S. Khan, A. Haque, M. K. Al-Suti, P. R. Raithby, *J. Organomet. Chem.* **2015**, *793*, 114.
[4] J. Granell, M. Martínez, *Dalton Trans.* **2012**, *41*, 11243.
[5] J. Dupont, C. S. Consorti, J. Spencer, *Chem. Rev.* **2005**, *105*, 2527.
[6] U. Fekl, K. I. Goldberg, *Adv. Inorg. Chem.* **2003**, *54*, 259.
[7] A. J. Canty, *Dalton Trans.* **2009**, 10409.
[8] M. Crespo, *Inorganics* **2014**, *2*, 115.
[9] M. Crespo, M. Font-Bardia, M. Martínez, *Dalton Trans.* **2015**, *44*, 19543.
[10] T. Calvet, M. Crespo, M. Font-Bardía, S. Jansat, M. Martínez, *Organometallics* **2012**, *31*, 4367.
[11] C. M. Anderson, R. J. Puddephatt, G. Ferguson, A. J. Lough, *J. Chem. Soc., Chem. Commun.* **1989**, *1297*.
[12] L. M. Rendina, R. J. Puddephatt, *Chem. Rev.* **1997**, *97*, 1735.
[13] M. Crespo, M. Martínez, S. M. Nabavizadeh, M. Rashidi, *Coord. Chem. Rev.* **2014**, *279*, 115.
[14] J. A. Labinger, J. E. Bercaw, *Nature* **2002**, *417*, 507.
[15] M. Albrecht, *Chem. Rev.* **2009**, *110*, 576.
[16] M. Crespo, *Organometallics* **2011**, *31*, 1216.

[17] T. Calvet, M. Crespo, M. Font-Bardia, K. Gómez, G. González, M. Martínez, *Organometallics* **2009**, *28*, 5096.

[18] T. Wang, J. A. Love, *Organometallics* **2008**, *27*, 3290.

[19] M. Jamshidi, M. Babaghasabha, H. R. Shahsavari, S. M. Nabavizadeh, *Dalton Trans.* **2017**, *46*, 15919.

[20] Á. Díez, E. Lalinde, M. T. Moreno, *Coord. Chem. Rev.* **2011**, *255*, 2426.

[21] M. Fereidoonnezhad, B. Kaboudin, T. Mirzaee, R. Babadi Aghakhanpour, M. Golbon Haghighi, Z. Faghih, Z. Faghih, Z. Ahmadipour, B. Notash, H. R. Shahsavari, *Organometallics* **2017**, *36*, 1707.

[22] M. Fereidoonnezhad, H. R. Shahsavari, S. Abedanzadeh, A. Nezafati, A. Khazali, P. Mastrorilli, M. Babaghasabha, J. Webb, Z. Faghih, Z. Faghih, S. Bahemmat, M. H. Beyzavi, *New J. Chem.* **2018**, *42*, 8681.

[23] F. Raoof, M. Boostanizadeh, A. R. Esmaeilbeig, S. M. Nabavizadeh, R. Babadi Aghakhanpour, K. B. Ghiassi, M. M. Olmstead, A. L. Balch, *RSC Adv.* **2015**, *5*, 85111.

[24] S. M. Nabavizadeh, H. Amini, F. Jame, S. Khosraviolya, H. R. Shahsavari, F. Niroomand Hosseini, M. Rashidi, *J. Organomet. Chem.* **2012**, *698*, 53.

[25] A. Nahaei, A. Rasekh, M. Rashidi, F. Niroomand Hosseini, S. M. Nabavizadeh, *J. Organomet. Chem.* **2016**, *815*, 35.

[26] M. Safa, R. J. Puddephatt, *J. Organomet. Chem.* **2014**, *761*, 42.

[27] P. V. Bernhardt, T. Calvet, M. Crespo, M. Font-Bardía, S. Jansat, M. Martínez, *Inorg. Chem.* **2012**, *52*, 474.

[28] F. Niroomand Hosseini, *Polyhedron* **2015**, *100*, 67.

[29] L. Maidich, A. Zucca, G. J. Clarkson, J. P. Rourke, *Organometallics* **2013**, *32*, 3371.

[30] M. Fereidoonnezhad, M. Niazi, M. Shahmohammadi Beni, S. Mohammadi, Z. Faghih, Z. Faghih, H. R. Shahsavari, *ChemMedChem* **2017**, *12*, 456.

[31] M. Fereidoonnezhad, H. R. Shahsavari, S. Abedanzadeh, B. Behchenari, M. Hossein-Abadi, Z. Faghih, M. H. Beyzavi, *New J. Chem.* **2018**, *42*, 2385.

[32] H. R. Shahsavari, R. B. Aghakhanpour, M. Fereidoonnezhad, *New J. Chem.* **2018**, *42*, 2564.

[33] H. R. Shahsavari, R. Babadi Aghakhanpour, M. Hossein-Abadi, R. Kia, P. R. Raithby, *Appl. Organomet. Chem.* **2018**, *32*, e4216.

[34] H. R. Shahsavari, R. Babadi Aghakhanpour, M. Babaghasabha, M. Golbon Haghighi, S. M. Nabavizadeh, B. Notash, *Eur. J. Inorg. Chem.* **2017**, *2017*, 2682.

[35] M. Niazi, H. R. Shahsavari, *J. Organomet. Chem.* **2016**, *803*, 82.

[36] M. E. Moustafa, P. D. Boyle, R. J. Puddephatt, *Organometallics* **2014**, *33*, 5402.

[37] S. Jamali, S. M. Nabavizadeh, M. Rashidi, *Inorg. Chem.* **2008**, *47*, 5441.

[38] G. Golbon Haghighi, M. Rashidi, S. M. Nabavizadeh, S. Jamali, R. J. Puddephatt, *Dalton Trans.* **2010**, *39*, 11396.

[39] M. Niazi, H. R. Shahsavari, M. Golbon Haghighi, M. R. Halvagar, S. Hatami, B. Notash, *RSC Adv.* **2016**, *6*, 76463.

[40] H. R. Shahsavari, R. B. Aghakhanpour, M. Babaghasabha, M. G. Haghighi, S. M. Nabavizadeh, B. Notash, *New J. Chem.* **2017**, *41*, 3798.

[41] T. E. Müller, D. M. P. Mingos, *Transition Met. Chem.* **1995**, *20*, 533.

[42] H. R. Shahsavari, R. Babadi Aghakhanpour, M. Hossein-Abadi, R. Kia, M. R. Halvagar, P. R. Raithby, *New J. Chem.* **2018**, *42*, 9159.

[43] S. Jamali, R. Czerwieniec, R. Kia, Z. Jamshidi, M. Zabel, *Dalton Trans.* **2011**, *40*, 9123.

[44] A. Zucca, L. Maidich, L. Canu, G. L. Petretto, S. Stoccoro, M. A. Cinellu, G. J. Clarkson, J. P. Rourke, *Chem. – Eur. J.* **2014**, *20*, 5501.

[45] C. Stoe, *X-AREA, version 1.30, program for the acquisition and analysis of data*, Stoe & Cie GmbH, Darmatadt **2005**.

[46] C. Stoe, *X–RED: program for data reduction and absorption correction, Version 1.28 b*, Stoe & Cie GmbH, Darmstadt **2005**.

[47] C. Stoe, *X-SHAPE, version 2.05, program for crystal optimization for numerical absorption correction*, Stoe & Cie GmbH, Darmstadt **2004**.

[48] G. M. Sheldrick, SHELX97: Program for Crystal Structure Solution, University of Göttingen, Germany, **1997**.

[49] C. Stoe, *X-STEP32, version 1.07 b, crystallographic package*, Stoe & Cie GmbH, Darmstadt **2000**.

[50] M. J. Frisch, G. W. Trucks, H. B. Schlegel, G. E. Scuseria, M. A. Robb, J. R. Cheeseman, G. Scalmani, V. Barone, B. Mennucci, G. A. Petersson, H. Nakatsuji, M. Caricato, X. Li, H. P. Hratchian, A. F. Izmaylov, J. Bloino, G. Zheng, J. L. Sonnenberg, M. Hada, M. Ehara, K. Toyota, R. Fukuda, J. Hasegawa, M. Ishida, T. Nakajima, Y. Honda, O. Kitao, H. Nakai, T. Vreven, J. J. A. Montgomery, J. E. Peralta, F. Ogliaro, M. Bearpark, J. J. Heyd, E. Brothers, K. N. Kudin, V. N. Staroverov, T. Keith, R. Kobayashi, J. Normand, K. Raghavachari, A. Rendell, J. C. Burant, S. S. Iyengar, J. Tomasi, M. Cossi, N. Rega, J. M. Millam, M. Klene, J. E. Knox, J. B. Cross, V. Bakken, C. Adamo, J. Jaramillo, R. Gomperts, R. E. Stratmann, O. Yazyev, A. J. Austin, R. Cammi, C. Pomelli, J. W. Ochterski, R. L. Martin, K. Morokuma, V. G. Zakrzewski, G. A. Voth, P. Salvador, J. J. Dannenberg, S. Dapprich, A. D. Daniels, O. Farkas, J. B. Foresman, J. V. Ortiz, J. Cioslowski, D. J. Fox, *Gaussian 09, Revision B.01*, Gaussian Inc., Wallingford, CT **2010**.

[51] P. J. Hay, W. R. Wadt, *J. Chem. Phys.* **1985**, *82*, 270.

[52] V. Barone, M. Cossi, J. Tomasi, *J. Chem. Phys.* **1997**, *107*, 3210.

[53] M. Cossi, G. Scalmani, N. Rega, V. Barone, *J. Chem. Phys.* **2002**, *117*, 43.

SUPPORTING INFORMATION

Additional supporting information may be found online in the Supporting Information section at the end of the article.

How to cite this article: Chamyani S, Shahsavari HR, Abedanzadeh S, Golbon Haghighi M, Shabani S, Notash B. Carbon-iodide bond activation by cyclometalated Pt (II) complexes bearing tricyclohexylphosphine ligand: A comparative kinetic study and theoretical elucidation. *Appl Organometal Chem*. 2018;e4674. https://doi.org/10.1002/aoc.4674